

# Isotopic production cross sections of residual nuclei in proton- and deuteron-induced reactions on $^{91,92}\text{Y}$ , $^{92,93}\text{Zr}$ , and $^{93,94}\text{Nb}$ around 100 MeV/nucleon

Yu. Watanabe<sup>a</sup>, J. Suwa<sup>a,b</sup>, K. Nakano<sup>a,b</sup>, S. Kawase<sup>a</sup>, H. Wang<sup>b</sup>, H. Otsu<sup>b</sup>, H. Sakurai<sup>b</sup>, D.S. Ahn<sup>b</sup>, M. Aikawa<sup>c</sup>, T. Ando<sup>d</sup>, S. Araki<sup>a,b</sup>, S. Chen<sup>b</sup>, N. Chiga<sup>b</sup>, P. Doornenbal<sup>b</sup>, N. Fukuda<sup>b</sup>, T. Isobe<sup>b</sup>, S. Kawakami<sup>f,b</sup>, T. Kin<sup>a</sup>, Y. Kondo<sup>e</sup>, S. Koyama<sup>d</sup>, S. Kubono<sup>b</sup>, Y. Maeda<sup>f</sup>, A. Makinaga<sup>g,h</sup>, M. Matsushita<sup>i</sup>, T. Matsuzaki<sup>b</sup>, S. Michimasa<sup>i</sup>, S. Momiyama<sup>d</sup>, S. Nagamine<sup>d</sup>, T. Nakamura<sup>e</sup>, M. Niikura<sup>d</sup>, T. Ozaki<sup>e</sup>, A. Saito<sup>e</sup>, T. Saito<sup>d</sup>, Y. Shiga<sup>j,b</sup>, M. Shikata<sup>e</sup>, Y. Shimizu<sup>b</sup>, S. Shimoura<sup>i</sup>, T. Sumikama<sup>b</sup>, P.A. Soderstrom<sup>b</sup>, H. Suzuki<sup>b</sup>, H. Takeda<sup>b</sup>, S. Takeuchi<sup>e</sup>, R. Taniuchi<sup>d</sup>, Y. Togano<sup>e</sup>, J. Tsubota<sup>e</sup>, M. Uesaka<sup>b</sup>, Ya. Watanabe<sup>b</sup>, K. Wimmer<sup>d,i,b</sup>, T. Yamamoto<sup>f,b</sup>, and K. Yoshida<sup>b</sup>

<sup>a</sup> Department of Advanced Energy Engineering Sciences, Kyushu University, Kasuga, Japan, <sup>b</sup> RIKEN Nishina Center, Wako, Japan, <sup>c</sup> Faculty of Science, Hokkaido University, Sapporo, Japan, <sup>d</sup> University of Tokyo, Tokyo, Japan, <sup>e</sup> Tokyo Institute of Technology, Tokyo, Japan, <sup>f</sup> University of Miyazaki, Miyazaki, Miyazaki, Japan, <sup>g</sup> JEI Institute for Fundamental Science, NPO Einstein, Kyoto, Japan, <sup>h</sup> Graduate School of Medicine, Hokkaido University, Sapporo, Japan, <sup>i</sup> Center for Nuclear Study, University of Tokyo, Wako, Saitama, Japan, <sup>j</sup> Department of Physics, Rikkyo University, Tokyo, Japan

## Abstract

Production cross sections of residual nuclei via proton- and deuteron-induced spallation reactions on  $^{91,92}\text{Y}$ ,  $^{92,93}\text{Zr}$ , and  $^{93,94}\text{Nb}$  at projectile energies around 100 MeV/nucleon were measured in inverse kinematics at the RIKEN Radioactive Isotope Beam Factory. Noticeable jumps in the measured cross sections of isotone production appear between the neutron numbers  $N=51$  and 50 for target nuclei with the initial neutron number  $N_{init}=53$  ( $^{92}\text{Y}$ ,  $^{93}\text{Zr}$ , and  $^{94}\text{Nb}$ ), while such jump is not clearly seen for target nuclei with  $N_{init}=52$  ( $^{91}\text{Y}$ ,  $^{92}\text{Zr}$ , and  $^{93}\text{Nb}$ ). The measured isotopic production cross sections are compared with PHITS calculations considering both the intranuclear cascade and evaporation processes in order to benchmark the reaction models.

## 1 Introduction

In recent years, a new research project has started for cross-section measurement of residues produced in  $p$ - and  $d$ -induced spallation reactions on long-lived fission products (LLFPs) (e.g.,  $^{79}\text{Se}$ ,  $^{93}\text{Zr}$  [1],  $^{107}\text{Pd}$  [2],  $^{126}\text{Sn}$ ,  $^{135}\text{Cs}$ ) using the inverse kinematics technique at RIKEN RI Beam Factory (RIBF) in order to accumulate basic data necessary for nuclear waste transmutation. In the isotopic distribution of the measured cross sections for  $^{93}\text{Zr}$  [1] at 105 MeV/nucleon, noticeable jumps at the neutron magic number  $N = 50$  were observed in the produced Zr and Y isotopes. In the  $^{93}\text{Zr}$  experiment, the secondary beams containing  $^{91,92}\text{Y}$ ,  $^{92,93}\text{Zr}$ , and  $^{93,94}\text{Nb}$  at kinetic energies around 100 MeV/nucleon were produced by in-flight fission of  $^{238}\text{U}$  at 345 MeV/nucleon on a beryllium target. Therefore, it is possible to extract isotopic-production cross sections of  $p$ - and  $d$ -induced spallation reactions on these nuclei except  $^{93}\text{Zr}$  by identifying the particles in the secondary beams in off-line data analysis.

In the present work, further data analysis of the  $^{93}\text{Zr}$  experiment has been performed and the cross sections for  $p$ - and  $d$ -induced spallation reactions on five nuclei adjacent to  $^{93}\text{Zr}$  (i.e.,  $^{91,92}\text{Y}$ ,  $^{92}\text{Zr}$ , and  $^{93,94}\text{Nb}$ ) have been obtained. Based on the systematic data, the behaviour of isotopic distribution of the measured cross sections is investigated with particular attention to the effect of neutron shell closure with  $N=50$  on the  $p$ - and  $d$ -induced spallation reactions. Moreover, the measured data are compared with model calculations using the Particle and Heavy Ion Transport code System (PHITS) [3] in order to benchmark the reaction models used in PHITS, namely, the Liège Intranuclear Cascade model (INCL) [4] and the generalized evaporation model (GEM) [5].

## 2 Experiment

The experiment was performed at RIBF. The details of the experimental procedure have been reported in Refs. [1, 2]. The secondary beam containing  $^{91,92}\text{Y}$ ,  $^{92,93}\text{Zr}$ , and  $^{93,94}\text{Nb}$  at kinetic energies around 100 MeV/nucleon was produced by in-flight fission of  $^{238}\text{U}$  at 345 MeV/nucleon on a 3 mm thick beryllium target in the first stage of the BigRIPS separator [6]. In the second stage of BigRIPS, the beam particles were selected and identified event-by-event using the  $B\rho$ -TOF- $\Delta E$  method [7]. Fig. 1 depicts the correlation plot of the mass-to-charge ratio  $A/Q$  and the proton number  $Z$  for the secondary beam.

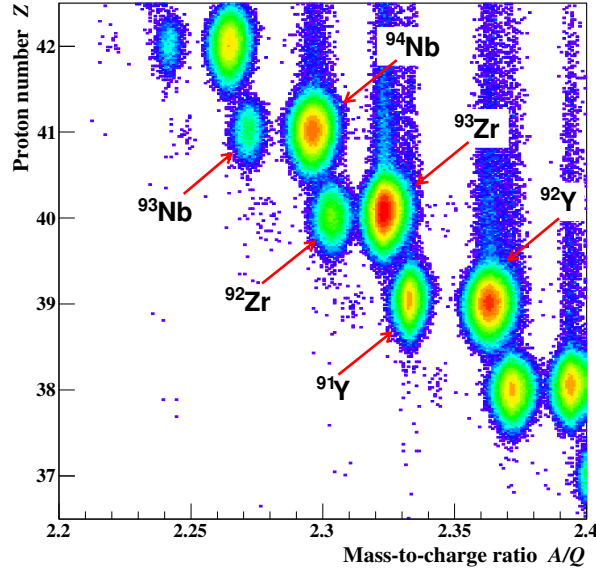


**Fig. 1:** Correlation plot of the proton number  $Z$  and the mass-to-charge ratio  $A/Q$  in BigRIPS.

Then, the beam particles bombarded the secondary targets,  $\text{CH}_2$ ,  $\text{CD}_2$ , and natural C placed at the entrance of the ZeroDegree Spectrometer (ZDS). The target thicknesses were 179.2, 218.2, and 226.0  $\text{mg}/\text{cm}^2$ , respectively. The residual nuclei produced by nuclear reactions in the second targets were analysed and identified event-by-event using the ZDS. Since the momentum acceptance of the ZDS is limited to  $\sim \pm 3\%$ , the experiment was carried out by using five different momentum settings ( $\Delta(B\rho)/B\rho = -9\%$ ,  $-6\%$ ,  $-3\%$ ,  $0\%$ , and  $+3\%$ ) for each target so as to accept the produced isotopes with a wide range of  $A/Q$ . Fig. 2 shows a correlation plot of  $A/Q$  and  $Z$  for the  $\Delta(B\rho)/B\rho = -6\%$  run in the ZDS used for particle identification after  $^{91}\text{Y}$  was selected in Fig. 1.

## 3 Results and Discussion

### 3.1 Experimental results

Figure 3 shows the measured isotopic production cross sections via the  $^{91}\text{Y}$  spallation reactions on proton and deuteron as an example. The black and red symbols denote proton-induced cross sections ( $\sigma_p$ ) and deuteron-induced cross sections ( $\sigma_d$ ), respectively. They were obtained from the measurements using the  $\text{CH}_2$  and  $\text{CD}_2$  targets, respectively, after the subtraction of contributions from carbon (using data from the C target run) and beam-line materials (using data from the empty-target run). The error bars include only the statistical uncertainties. The systematic uncertainties were estimated in accordance with Ref. [1]: the target thickness ( $\leq 2\%$ ) and the charge state distributions in ZDS ( $5\%$ ).

In Fig. 3,  $\sigma_p$  is found to be approximately twice as large as  $\sigma_d$  for Zr isotopes produced by charge-

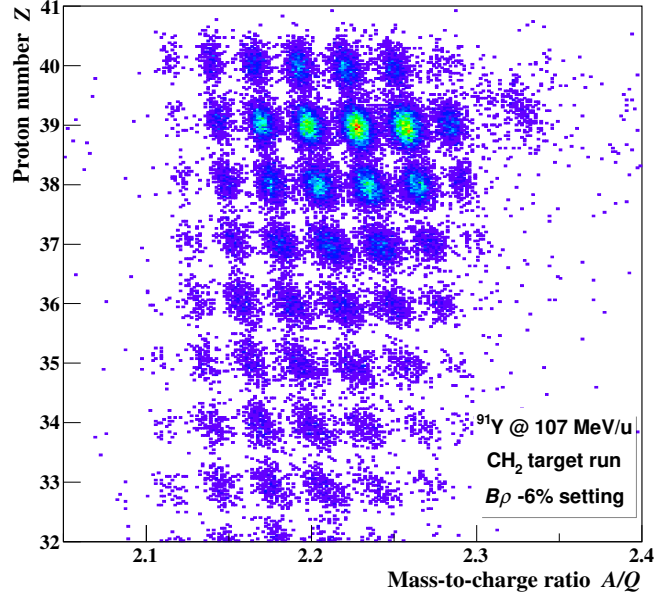


**Fig. 2:** Correlation plot of the proton number  $Z$  and the mass-to-charge ratio  $A/Q$  in ZDS.

increasing reactions, and  $\sigma_p$  and  $\sigma_d$  are almost identical for Y isotopes produced by charge-unchanging reactions. Meanwhile,  $\sigma_d$  becomes large compared to  $\sigma_p$  as the atomic number decreases from Sr to Br. The observed trends are the same as in the results of  $^{93}\text{Zr}$  [1] and  $^{107}\text{Pd}$  [2]. In the case of  $^{93}\text{Zr}$  [1], characteristic jump structure near  $N=50$  was observed in the isotopic distribution for the elements corresponding to charge-unchanging ( $\Delta Z = 0$ ) and one-proton-removal ( $\Delta Z = -1$ ). However, no discontinuous change in the cross section is observed in Y isotopes produced in the reactions  $^{91}\text{Y} + p$  and  $d$  as shown in Fig. 3, while a jump is seen in the production of isotopic chains between  $^{88}\text{Sr}$  and  $^{89}\text{Sr}$  in the  $^{91}\text{Y} + p$  reaction.

To investigate the effect of neutron shell closure with  $N = 50$ , we have obtained the isotone production cross sections, namely, the production cross sections of residual nuclei with the same neutron number  $N$ . The isotone production cross sections are plotted as a function of  $N$  for six nuclei in Fig. 4. The six nuclei are divided into the two groups according to the initial neutron number  $N_{init}$ . The upper panel presents the results of nuclei with  $N_{init}=52$  (i.e.,  $^{91}\text{Y}$ ,  $^{92}\text{Zr}$ , and  $^{93}\text{Nb}$ ), and the lower panel corresponds to the result of nuclei with  $N_{init}=53$  (i.e.,  $^{92}\text{Y}$ ,  $^{93}\text{Zr}$ , and  $^{94}\text{Nb}$ ). In the lower panel, the distributions look very similar among the three nuclei with  $N_{init}=53$ . The measured cross sections have characteristic shoulders at  $N=52$  and relatively large jumps are seen between  $N=51$  and 50, which is considered as a signature of the effect of neutron shell closure with  $N = 50$ . On the other hand, the cross sections show a monotonic decrease with change in the neutron number from 50 to 52 in the upper panel, and such jumps as observed in the lower panel are not clearly seen between  $N=51$  and 50. The similar behaviour of isotone production was observed in  $d$ -induced reactions as well. Further consideration accompanied with theoretical model analyses will be necessary to clarify why the distributions of measured isotone production cross sections are different between  $N_{init}=52$  and 53.

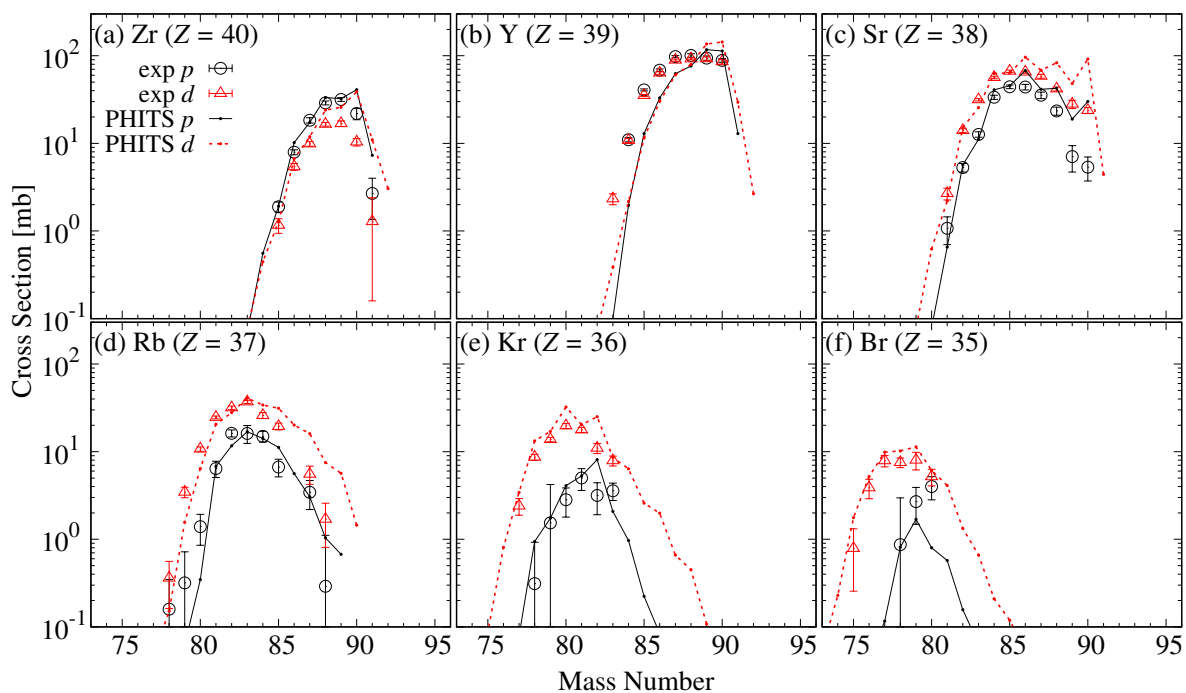


**Fig. 3:** Isotopic production cross section for the spallation reactions  $^{91}\text{Y} + p$  and  $d$  as a function of mass number for each isotope in the experimental acceptance: (a) Zr, (b) Y, (c) Sr, (d) Rb, (e) Kr, and (f) Br.

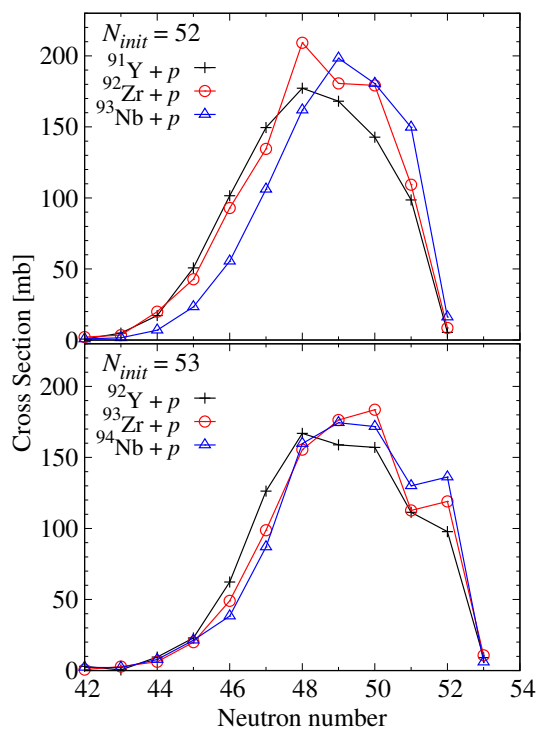


**Fig. 4:** Experimental cross sections of isotone production as a function of neutron number  $N$  for  $^{91}\text{Y}$ ,  $^{92}\text{Zr}$ , and  $^{93}\text{Nb}$  (upper panel) and  $^{92}\text{Y}$ ,  $^{93}\text{Zr}$ , and  $^{94}\text{Nb}$  (lower panel).

### 3.2 Comparison with theoretical model calculation

The spallation reactions have been well described as a two-step process, namely, the formation of pre-fragments via the intranuclear cascade process and the de-excitation process of the pre-fragments by evaporation of light particles. As in our previous works [1,2], we have used INCL 4.6 [4] and GEM [5] for the cascade and evaporation processes, respectively, in the present work. These models are implemented in PHITS [3].

The lines in Fig. 3 denote the cross sections calculated with PHITS. The black solid line and the red dashed line correspond to the  $p$ - and  $d$ -induced production cross sections ( $\sigma_p$  and  $\sigma_d$ ), respectively. The overall behaviour of the cross section is well reproduced by the PHITS calculation. However, there are some discrepancies between the measured and calculated cross sections. For Zr-isotope, the calculation cannot explain the twofold difference between  $\sigma_p$  and  $\sigma_d$ . The calculated  $\sigma_p$  and  $\sigma_d$  for Y-isotopes underestimate the measured ones substantially in the neutron deficient region. The PHITS calculation overestimates the measured  $\sigma_p$  and  $\sigma_d$  in the neutron rich region for Zr, Y, and Sr isotopes. As discussed in Ref. [1], this overestimation is partly due to inappropriate treatment of the intranuclear cascade process in the peripheral region in INCL. In addition, the even-odd staggering seen in the calculated cross sections is exaggerated in Rb and Kr isotopes. Similar discrepancies were seen in the benchmark test of PHITS for  $p$ - and  $d$ -induced spallation reactions on  $^{93}\text{Zr}$  [1] and  $^{107}\text{Pd}$  [2]. Thus, further study will be required toward improvement of the INCL and GEM models.

## 4 Summary and Conclusions

We have measured systematically the production cross sections of residual nuclei in proton- and deuteron-induced reactions on  $^{91,92}\text{Y}$ ,  $^{92,93}\text{Zr}$ , and  $^{93,94}\text{Nb}$  at projectile energies around 100 MeV/nucleon. Noticeable jumps in the measured cross sections of isotone production were observed between  $N=51$  and 50 for target nuclei with the initial neutron number  $N_{init}=53$  ( $^{92}\text{Y}$ ,  $^{93}\text{Zr}$ , and  $^{94}\text{Nb}$ ), while the similar jumps were not clearly seen for target nuclei with  $N_{init}=52$  ( $^{91}\text{Y}$ ,  $^{92}\text{Zr}$ , and  $^{93}\text{Nb}$ ). The measured isotopic production cross sections for  $^{91}\text{Y}$  were compared with the PHITS calculations with INCL 4.6 for the intranuclear cascade process and GEM for the evaporation process. Although the PHITS calculations were in overall good agreement with the measured cross sections, some discrepancies to be improved were found: *e.g.*, overestimation in neutron-rich side, exaggerated even-odd staggering, and so on. We will continue to investigate the effect of neutron shell closure on  $p$ - and  $d$ -induced spallation reactions along with further improvement of the reaction models.

## Acknowledgements

We are grateful to the accelerator staff of the RIKEN Nishina Center for providing a high-quality  $^{238}\text{U}$  beam. This work was funded by ImPACT Program of Council for Science, Technology and Innovation (Cabinet Office, Government of Japan).

## References

- [1] S. Kawase *et al.*, *Prog. Theor. Exp. Phys.* **2017** (2017) 093D03.
- [2] H. Wang *et al.*, *Prog. Theor. Exp. Phys.* **2016** (2016) 021D01.
- [3] T. Sato *et al.*, *J. Nucl. Sci. Technol.*, **50** (2013) 913.
- [4] A. Boudard *et al.*, *Phys. Rev. C* **87** (2013) 014606.
- [5] S. Furihata, *Nucl. Instrum. Meth. B* **171** (2000) 251.
- [6] T. Kubo *et al.*, *Prog. Theor. Exp. Phys.* **2012** (2012) 03C003.
- [7] N. Fukuda *et al.*, *Nucl. Instrum. Meth. B.* **317** (2012) 323.

